

DOKUZ EYLÜL UNIVERSITY
GRADUATE SCHOOL OF NATURAL AND APPLIED SCIENCES

**DIRECTION OF ARRIVAL ESTIMATION BY
USING STANDARD COMMUNICATION
TECHNOLOGIES IN INDOOR ENVIRONMENT**

by
Suat YETİŞ

October, 2018
İZMİR

**DIRECTION OF ARRIVAL ESTIMATION BY
USING STANDARD COMMUNICATION
TECHNOLOGIES IN INDOOR ENVIRONMENT**

**A Thesis Submitted to the
Graduate School of Natural and Applied Sciences of Dokuz Eylül University
In Partial Fulfillment of the Requirements for the Degree of Master of Science
in Mechatronics Engineering Program**

**by
Suat YETİŞ**

**October, 2018
İZMİR**

M.Sc THESIS EXAMINATION RESULT FORM

We have read the thesis entitled “**DIRECTION OF ARRIVAL ESTIMATION BY USING STANDARD COMMUNICATION TECHNOLOGIES IN INDOOR ENVIRONMENT**” completed by **SUAT YETİŞ** under supervision of **ASST. PROF. DR. ÖZGÜR TAMER** and we certify that in our opinion it is fully adequate, in scope and in quality, as a thesis for the degree of Master of Science.

Asst. Prof. Dr. Özgür TAMER

Supervisor

Dr. Öğretim Üyesi Talan İSİTİR

(Jury Member)

Dr. Öğretim Üyesi Ahmet ÖZKURT

(Jury Member)

Prof.Dr. Kadriye ERTEKİN

Director
Graduate School of Natural and Applied Sciences

ACKNOWLEDGEMENTS

A special note of thanks goes to my supervisor Asst. Prof. Dr. Özgür TAMER for his guidance, comments and support at every point of this study. Without his support and consideration, this dissertation would have never been completed.

I would like to show gratitude to my dearest friends Türker & İlke TÜRKORAL, for sharing the good and bad times and supporting me.

I would like to express my deepest gratitude to my family. Thank you for always believing in me from the very beginning and your continuous emotional support; giving me strength.

Lastly but not less, I would like to thank you to my lovely girlfriend Gözde BİLGİN, her patience and motivate me all the time.

This work has been supported by The Scientific and Technological Research Council of Turkey (TUBITAK) under Grant No. 114E659.

Suat YETİŞ

DIRECTION OF ARRIVAL ESTIMATION BY USING STANDARD COMMUNICATION TECHNOLOGIES IN INDOOR ENVIRONMENT

ABSTRACT

Recently, direction of arrival estimation has become a significant information to obtain the position of mobile devices which they have wireless communication technologies. The accuracy of the direction of arrival (DOA) estimation has a crucial role to determine the position of these devices, such as robots, vehicles etc. An antenna array structure makes possible to estimate direction of arrival angle by using the several array signal processing techniques. The primary aim of this study to obtain the DOA estimation and can be applied with any distance position techniques, for using in low-profile devices to acquire 1-D indoor position of mobile devices. The multiple signal classification method is almost used with all geometric array configurations to determine the direction of arrival angle of the incoming signal. In this dissertation, we will apply MUSIC algorithm one by one to the uniform linear array, the uniform circular array and the L-shaped array geometric configurations. Moreover, we perform a MATLAB based simulation to combine all the results, to improve the accuracy of the DOA estimations.

Keywords: Direction of arrival estimation, multiple signal classification, uniform linear array, uniform circular array, L-shaped array, mobile devices

STANDART HABERLEŐME TEKNOLOJİLERİ KULLANILARAK KAPALI ALANLARDA GELİŐ AÇISI KESTİRİMİ YAPILMASI

ÖZ

Geliő açısı kestirim bilgisi; kablosuz iletiőim teknolojisini kullanan mobil cihazların konumlarının belirlenmesinde önemli bir veri haline gelmiőtir. Robotlar ve araçlar gibi mobil cihazların pozisyonlarının dođru bir Őekilde elde edilmesi iin, geliő açısı kestirim bilgisinin hassasiyeti de önemli rol almaktadır. Geliő açısı kestirimi; bir anten dizisi ile birlikte uygun bir sinyal iŐleme tekniđi kullanılarak elde edilebilir. Bu alıŐmanın temel amacı; dűŐük profilli mobil cihazların konumlarının belirlenmesinde, herhangi bir mesafe belirleme tekniđi ile birlikte kullanılabilcek tek boyutlu dűzlemde geliő açısı kestirim bilgisi elde etmektir. oklu sinyal sınıflandırma tekniđi; gelen sinyal geliő açısını elde etmek iin, hemen hemen bűtűn geometrik anten dizilerine uygulanmıŐtır. Bu alıŐmamızda, oklu sinyal sınıflandırma yöntemini dođrusal, dairesel ve L Őeklinde geometrik yapıya sahip anten dizilerine uygulayarak geliő açısı kestirim verisini elde edilmiőtir. Ayrıca, MATLAB tabanlı benzetimler geliŐtirerek, tűm geometrik anten dizilerinden gelen verileri sentezleyip, geliő açısı kestirim bilgisinin dođruluđu artırılmıŐtır.

Anahtar kelimeler: Geliő açısı kestirimi, oklu sinyal sınıflandırma, dođrusal anten dizisi, dairesel anten dizisi, L-Őeklinde anten dizisi, mobil cihazlar

CONTENTS

	Page
M.Sc THESIS EXAMINATION RESULT FORMHata! tanımlanmamış.	Yer işareti
ACKNOWLEDGEMENTS	ii
ABSTRACT	iii
ÖZ	iv
LIST OF FIGURES	vii
LIST OF TABLES	viii
CHAPTER ONE - INTRODUCTION	1
CHAPTER TWO – DIRECTION OF ARRIVAL ESTIMATION	7
2.1 Signal Model	7
2.2 Array Construction.....	8
2.2.1 Array Response of Uniform Linear Array.....	8
2.2.2 Array Response of Uniform Circular Array	10
2.2.3 The Steering Matrix of L-Shaped Array.....	13
2.3 Properties of Subspace DOA Methods	14
2.3.1 Multiple Signal Classification Method.....	14
CHAPTER THREE - METHODOLOGY	17
3.1 Implementation of MUSIC Algorithm for ULA Configuration	17
3.2 Implementation of MUSIC Algorithm for the ULSA Configuration	19
3.3 Applying MUSIC Algorithm to UCA Configuration	20
3.4 Determining DOA by Applying Multiple Algorithm via Their Error Weight Function	23
CHAPTER FOUR - RESULTS	25
4.1 Simulation Result of ULA Configuration.....	25

4.2 Simulation Result of ULSA Configuration.....	27
4.3 Simulation Result of UCA Configuration.....	28
4.3.1 Simulation Results of the UCA Structure for Single Source Receiving Signal.....	28
4.3.2 Simulation Results of the UCA Structure for Two Source Receiving Signal	30
4.4 Comparing ULA, ULSA and UCA structures	33
CHAPTER FIVE - CONCLUSION	35
REFERENCES.....	36
APPENDICES	42

LIST OF FIGURES

	Page
Figure 1.1 The simple view of the robot which is used in implementations	6
Figure 1.2 Basic geometrical structure of antenna locations	6
Figure 2.1 Overview of Direction of Arrival Estimation.....	7
Figure 2.2 Uniform linear array model via azimuth angle.....	8
Figure 2.3 Uniform circular array model on polar rectangular coordinates	10
Figure 2.4 L-Shaped Array geometric structure	13
Figure 3.1 Uniform linear array configuration which consist two elements.....	17
Figure 3.2 The flow chart of the DOA estimation for ULA structure.	17
Figure 3.3 The ULSA geometric structure in our implementation.	19
Figure 3.4 Uniform circular array configuration with four elements.....	20
Figure 3.5 The flow chart of the DOA estimation for ULA structure.	17
Figure 3.6 Put on all the DOA configurations in same scale.	23
Figure 4.1 Simulation for $\phi=44$, Trials=100, Snapshots=1000 and SNR=0 to 16	25
Figure 4.2 Trials = 25, Snapshots=1000, SNR=20, DOA=-70 to 70 Degree	26
Figure 4.3 The Spatial Music Spectrum When the DOA=-85	26
Figure 4.4 The Relation of the SNR and the error estimation of the ULSA structure	27
Figure 4.5 The DOA estimations for the ULSA structure (DOA =10o-80o)	27
Figure 4.6 The spatial MUSIC spectrum of the ULSA when DOA=7o	28
Figure 4.7 The Performance of the UCA structure When SNR is -12 to 12.....	29
Figure 4.8 The Error values of the DOA estimations When DOA=10-35o	29
Figure 4.9 The error value of the estimations, when $\phi=350-360$ and $\phi=0-10$ degree	30
Figure 4.10 The MUSIC spectrum for two impinging signals with high resolution. .	31
Figure 4.11 The MUSIC spectrum for two impinging signals with low resolution. .	31
Figure 4.12 The histogram of the estimations when SNR=10 the snapshots=20000	33
Figure 4.13 Comparing the DOA estimations for combined. average and UCA error	33
Figure 4.14 Comparing the performance of the ULA, ULSA, UCA by SNR.....	34
Figure 4.15 Comparing the performance of the ULA, ULSA, UCA by angles.....	34

LIST OF TABLES

	Page
Table 4.1 The Result of 2 DOA Estimation for UCA Configuration	32



CHAPTER ONE

INTRODUCTION

In recent years, the development of the robotic technology has led to widespread uses of robots in many industrial and daily life applications. In some particular task domains, robots can perform tasks more economically and reliably than humans (Trinh, Duc Thang, Kim, Lee, & Chang, 2012). However, robots must have some information to achieve their tasks with high accuracy. Robot localization has been accepted as one of the most primary information (Borenstein, Everett, & Feng, 1996). Localization problem can be defined as determining the position of a robot, in mobile robotics (Cox, 1990). Moreover, position information is essential for controlling, tracking and monitoring of tasks assigned to robots.

Recently, many studies have been presented to specify the position of robot. Although plenty of proposed solutions are presented, in terms of developing a low-cost and fast technic for multiple-source signals, the robot localization problem is still a challenge. Global positioning system (GPS) is a good solution to determine position of devices, vehicles, robots etc., when they operate in an outdoor environment. GPS hasn't enough accuracy and sometimes it is completely useless, because of signal losses and corruption in indoor environments (Thummalapalli, 2012). That's why we need other technologies to find the position of a robot in an indoor environment. The robot odometric sensors are one of the solution to determine position of wheeled robots, as they give knowledge about robot movements. In this wise, if the initial position is known last position can be calculated. Unluckily, odometric sensors have some noise and accumulate errors in time (Borenstein & Feng, 1994). Because of that they aren't suitable for long term localization. Some techniques are developed to increase the accuracy, but these techniques cannot handle to decrease error in acceptable level for long time using (Wawak, Matia, Peignot, & Puente, 1999).

Wi-Fi based localization systems can be separated by the measurement techniques. These approaches are different from each other in terms of the specific technique used to sense and measure the position of the mobile device under the environmental

conditions. Basically, Real Time Location Systems (RTLS) can be classified into four categories (Cisco, 2008);

- Cell of origin (nearest cell)
- Distance (Lateration, tri-lateration, triangulation etc.)
- Angle (angulation, angle of arrival (AOA), direction of arrival (DOA))
- Location patterning (pattern recognition)

One or more of these techniques can be used together to design an RTLS system. Compared to distance based techniques; DOA estimation components are more expensive and their power consumption is higher. However, distance based techniques aren't convenient to be used in inhomogeneous mediums like underwater, indoor environment etc. (Zekavat & Buehrer, 2011).

Recently, direction of arrival estimation (DOA) emerge as an important data to determine the position of mobile robots which has more than one wireless components, such as wireless sensor networks. The DOA estimation and one distance technique like triangulation can be used together to obtain the position of a signal source. The accuracy of the direction of arrival estimation is significant in many areas like communication and radar systems including sonar, radio astronomy, and navigation systems (Hwang, Aliyazicioglu, Grice, & Yakovlev, 2008; Evans, Johnson, & Sun, 1982). Antenna array geometrical model and an efficient signal processing method can improve the performance and accuracy of DOA estimation (Lee, Chen, Song, Wei, & Hwang, 2005).

There is one-to-one relationship between the direction of a signal and the related received steering vector, that being so an antenna array can be used to estimate the direction of arrival information. An antenna array is formed by antennas that outspread in an area (Koca, 2015). They help to reduce interference, system complexity and to manipulate receiving signals for augmentation and parameter estimation in systems that they used (Johnson, 1982; Balanis & Ioannides, 2007).

Practically, the DOA estimation is made difficult by the fact that there is unknown number of impinging signals on the array at the same time and each of them are coming from unknown direction with unknown amplitudes. In addition, the received signals are always corrupted by the additive noise. Nonetheless, there are several techniques to estimate arrival angle of the impinging signals. The most commonly used DOA estimation techniques are spectrum based methods. The DOA can be obtained by spectral estimations methods by determining local maximums of signals from their spatial spectrum (Johnson, 1982). DOA estimation techniques can be categorized into two classes namely conventional techniques and subspace-based techniques (Balanis & Ioannides, 2007). Conventional techniques are also known as nonparametric techniques. Bartlett (1950), Capon (1969) and Burg (1967) developed some conventional-based algorithms to obtain DOA estimation (Bartlett, 1950; Capon, 1969; Burg, 1967). Tan et. al. (2002) presented that the algorithm of Burg; Maximum-likelihood estimation has better performance than others (Tan et. al., 2002). It maximizes log-likelihood function of incoming signal data to obtain DOA estimation. However, the conventional beamforming methods are useless when the angular space between the arriving signals are less than beam width (Haykin, 1985). In 1970s, some subspace-based techniques were developed. Multiple Signal Classification (MUSIC) are introduced by Schmidt (1986), and Roy and Kailath (1989) found out Estimation of Signal Parameters via Rotation Invariance (ESPRIT) algorithm (Schmidt, 1986; Roy & Kailath, 1989).

Several direction finding techniques and algorithms have been built to improve direction of arrival estimation in last years. Also, these algorithms were applied on different antenna array geometries. Bartlett, Capon, Maximum-likelihood, MUSIC and ESPRIT methods were firstly applied for uniform linear array (ULA) and uniform rectangular array (URA). Except Maximum-likelihood (ML) algorithm, the all of other techniques have been failed to determine angle of arrival for coherent signals (Wax & Sheinvald, 1994). Evans et. al. (1982) and Shan et. al. (1985) proposed spatial smoothing techniques to use with coherent signals in antennas which has ULA geometry (Evans, Johnson, & Sun, 1982; Shan, Wax, & Kailath, 1985). But, ULA can't provide full azimuth angle coverage and URA has same problem when non-

omnidirectional elements are used. The DOA estimation for uniform circular arrays (UCAs) and L-shaped arrays (LSA) has been developed in these scenarios.

Many two-dimensional (2D) angle of arrival estimation methods using planar arrays have been proposed. L-shaped array has been used one of the most widespread and its estimation performance is better than other geometric structure arrays (Liu, Yang, Li, & Cao, 2017). Many direction of arrival estimation techniques were applied L-shaped array geometry to improve its performance. MUSIC (Hua, Sarkar, & Weiner, 1989), ESPRIT (Jian, Shu-xun, & Xiao-li, 2006), Propagator Method (PM) (Tayem & Kwon, 2005) and Joint Singular Value Decomposition (JSVD) algorithm (Gu & Wei, 2007) were proposed. All these algorithms have been considered that L-shape array is formed by combining two uniform linear arrays (ULA). That's why the DOA estimation fidelity is limited by the array aperture (Liu, Yang, Li, & Cao, 2017). To overcome these problems some other algorithms like minimum-redundancy array (MRA) (Camps, Cardama, & Infantes, 2001), and two-level nested array (Pal & Vaidyanathan, 2010), were developed.

Another geometric structure of planar antenna array is circular array, which is used to estimate direction of arrival angle. In many applications the antenna is placed with uniform distance and the structure is called a uniform circular array (UCA). UCA has attracted more attention than other geometries recently, because it has some advantages like full coverage azimuth angle and a certain degree of elevation angle. In addition, the direction patterns synthesized with UCAs can be electronically rotated in the plane of array without considerable change of beam shape (Ioannides & Balanis, 2005; Lau & Leung, 2000). Moreover, all sensors on a circular array almost generates identical beam patterns because the UCA has no edge elements. Like all other geometrical structures plenty of the DOA techniques was applied to UCA. However, the UCA array manifold has not Vandermonde structure and more complex than other array type. The UCA steering vector needs a transformation technique to convert array manifold Vandermonde structure to get high performance with subspace methods. The UCA steering vectors are transformed to Vandermonde form via using phase mode excitation (Davies, 1983) by Doron & Doron (M.A. Doron & E. Doron, 1992). The

same direction of arrival methods, which are developed for other array structures such as MUSIC, were expanded for UCA geometry like UCA-MUSIC (Mathews & Zoltowski, 1994a), UCA-ESPRIT (Mathews & Zoltowski, 1994b), and their variations (Wax & Sheinvald, 1994; Chan & Litva, 1995).

In this thesis deals we propose a system to determine the DOA estimation and can be applied with any distance position techniques, for using in low-profile devices to obtain one-dimensional indoor position of mobile robots. The robots which we use in that thesis can be seen in Figure 1.1. The array antenna which we used has only four elements in a square form. We will apply different DOA algorithms to different variations of antenna array geometries without changing the location and number of elements. We will use different antennas variation to change array type. In Figure 1.1, it can be seen basic structure of our design. In that structure many array type can be created. We consider 3 types of array which they are uniform linear array (UCA), L-Shaped array (LSA) and uniform circular array (UCA). ULA is formed by antenna-1 and antenna-2, LSA is created by antenna-1, antenna-2 and antenna-4. UCA is comprised by all antennas. We applied MUSIC algorithm to determine DOA estimation on these three array structures. After determining DOA, we obtain weight for each results depending on their performance.

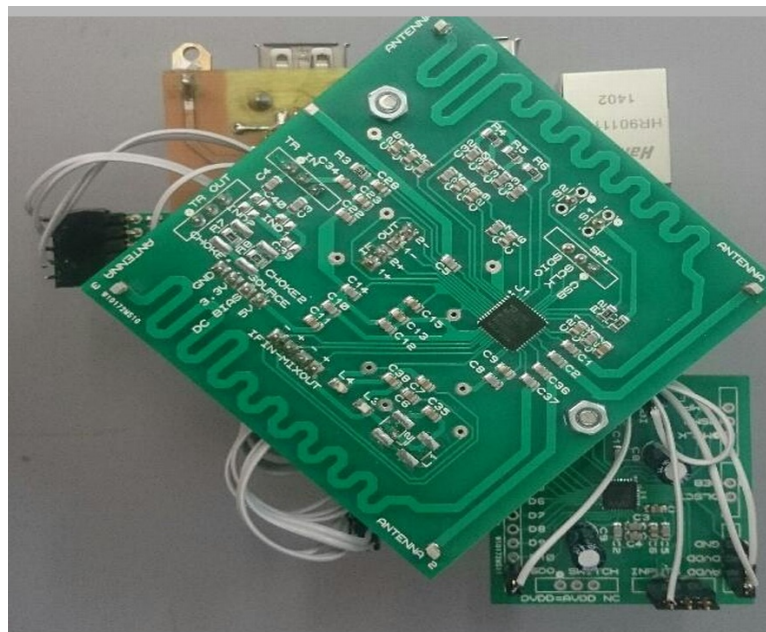


Figure 1.1 The simple view of the robot which is used in implementations

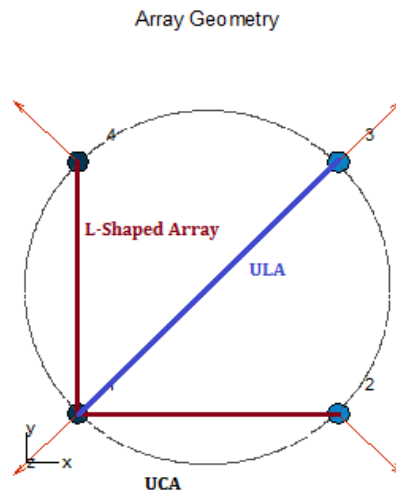


Figure 1.2 Basic geometrical structure of antenna locations

In the following chapter some principal concept to develop a subspace based DOA algorithms and their mathematical model for ULA, L-Shape, and UCA antenna array geometries are introduced. In the 3rd chapter the principle of MUSIC DOA algorithms for these three array types are discussed. In 4th chapter, the MATLAB simulation of DOA algorithms are presented and the performance for each scenario is analyzed. In chapter 5th conclusion is made and the possible future work is discussed.

CHAPTER TWO

DIRECTION OF ARRIVAL ESTIMATION

The purpose of DOA estimation is to estimate arrival angle of the impinging signal on an antenna array. The array geometry is very important in DOA estimation techniques. Also, each array type has some advantages and at the same time some disadvantages when we compare them. The antenna elements can be arranged in many geometries such as linear, circular planar and random arrays. In this chapter, ULA, LSA and UCA based DOA estimation will be introduced based on MUSIC algorithm.

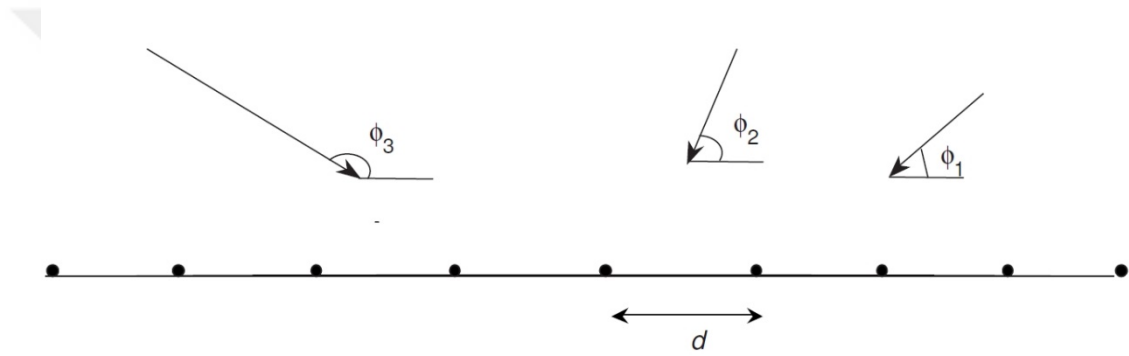


Figure 2.1 Overview of Direction of Arrival Estimation (Mubeen, Prasad, & Jhansi Rani, 2012)

2.1 Signal Model

Currently all the DOA estimation methods are model based. Proper mathematical model of signals and some assumptions (such as far field, narrowband assumption) have to be set up to apply the DOA estimation algorithms successfully. Basically signal impinging on an array can be modelled like below;

Consider an array composed of M elements and p receiving signals from different directions, $\Phi_1, \Phi_2, \dots, \Phi_p$. If the array output signal based on q number of snapshots is denoted by $x(t_1), x(t_2), \dots, x(t_q)$, then the $M \times 1$ observed data vector is:

$$x(t) = \sum_{k=1}^p \alpha(\Phi_k) s_k(t) + n(t), \quad t = t_1, t_2, \dots, t_q \quad (2.1)$$

Equation (2.1) in matrix notation is;

$$X = A.S + N \quad (2.2)$$

where the dimension of array output signal X is $M \times q$, A is the steering matrix of the array with dimension $M \times p$, S is the signal matrix with dimension $p \times q$ and N is the noise matrix with the same dimension of the array output signal $M \times q$.

2.2 Array Construction

In this section, we will construct signal model for Uniform Linear Array (ULA), Uniform Circular Array (UCA) and L-Shaped Array geometric structures. Many investigations have been done in the ULA already. Nearly all the DOA methods are implemented on this array structures. Nowadays, UCA geometry get more and more attention. Because it has some advantages compare to ULA and LSA (Zou, 2012).

2.2.1 Array Response of Uniform Linear Array

Consider a ULA consisting of M number of element that are aligned and equal spaced place on a line. The distance between elements is represented as d . In the noiseless medium, the signal that impinging on the rightmost element from the far-field source is denote as $s(t)$. In Figure 2.2 an ULA that is constructed by the M elements and a signal source is emitting from far-field is presented.

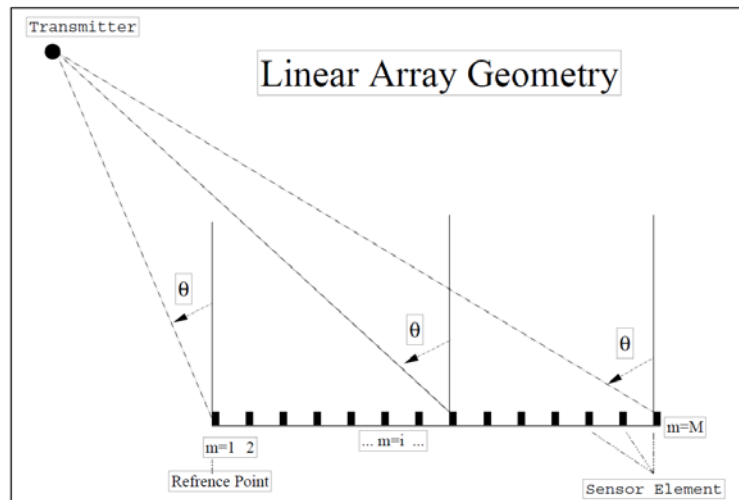


Figure 2.2 Uniform linear array model via azimuth angle (Shapoury, 2007)

The signal impinging on other elements will have some delays compared to rightmost element.

$$s_k(t) = s(t - \tau_k) \quad (2.3)$$

where τ_k is the relative delay between k^{th} element and the rightmost one.

The angle between the source and the line to ULA is defined as the direction of arrival. It is represented as Φ . Then the delay at m^{th} elements is presented as:

$$\tau = (m - 1) \frac{d \sin(\Phi)}{v} \quad (2.4)$$

When the ULA is constructed, the distance should be setup properly to avoid spatial aliasing. In other word, the phase difference between adjacent elements should not be more than π . If the phase difference larger than π , the phase delay can be the same as the one with $2\pi - \Phi$. To avoid spatial aliasing, the distance should be arranged with considering Equation 2.4;

$$\left| \frac{2\pi f d \sin \Phi}{v} \right| \leq \pi \quad (2.5)$$

The wavelength is determined by the maximum frequency of the signal, so;

$$\lambda_{min} = \frac{v}{f_{max}} \quad (2.6)$$

If we rearrange Equation 2.5;

$$d \leq \frac{\lambda}{2|\sin \Phi|} \quad (2.7)$$

where v , is the speed of the signal and d is the distance between adjacent elements.

Now we can write the antenna array response $A(\Phi)$ to the impinging s_k as

$$A(\Phi) = [\alpha_1(\Phi_1) \ \alpha_2(\Phi_2) \ \dots \ \alpha_p(\Phi_p)] \quad (2.8)$$

$$\alpha(\Phi) = [1, e^{-j(\frac{2\pi}{\lambda})d \cos \Phi}, \dots, e^{-j(\frac{2\pi}{\lambda})d(M-1) \cos \Phi}]^T \quad (2.9)$$

In section 2.1 the signal model of output signal was explained. After determining array steering vector, the array output signal can be written as below;

$$X(t) = A(\theta)s_k(t) + N(t) \quad (2.10)$$

In equation 2.10, $X(t)$ stands for received signal model, $N(t)$ represent the noise of the incoming signal.

In the case of the ULA geometric configuration, the steering vector of the incoming signal has Vandermonde Structure. Because of that, the MUSIC algorithm which is described in section 2.3.1, can be applied directly to estimate DOA information.

2.2.2 Array Response of Uniform Circular Array

As it can be seen in Figure 2.3, uniform circular array is a special planar array with some superb features over uniform linear array it is azimuthally coverage 360° . Moreover, it is a two-dimensional method which it can provide particular degree of elevation information. In addition, UCA usually needs less space than ULA. Practically, some hardware is very complex that leave a little space to place array. In this case, UCA will be a better option than ULA.

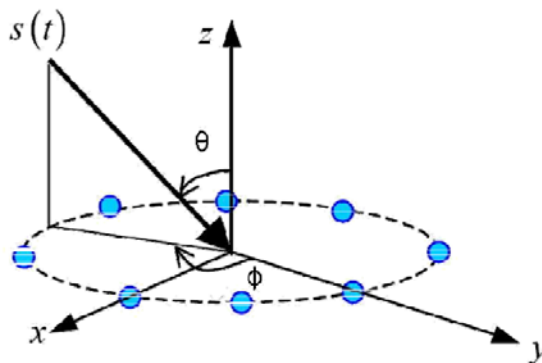


Figure 2.3 Uniform circular array model on polar rectangular coordinates (Al Jabr, Kwon, & Tayem, 2008)

The M identical antenna elements are distributed uniformly over the circumference of a circle with the radius r . If the center of the UCA point is taken as the reference

point, the signal of wavelength λ which is arriving from the azimuth angle $\phi \in [-\pi, \pi]$ and the elevation angle $\theta \in [0, \frac{\pi}{2}]$, then the n^{th} component of the steering vector can be obtained by Equation 2.11.

$$\alpha_n(\phi) = \exp[jkr \sin(\theta) \cos(\phi - \frac{2\pi(n-1)}{M})] \quad (2.11)$$

where k is named as the wave number. If we assume that $\zeta = k_0 r \sin \theta$, $\gamma_n = \frac{2\pi(n-1)}{M}$ and $n = (1, 2, \dots, M)$. The steering vector can be rearranged as:

$$\alpha(\phi) = [e^{j\zeta \cos(\phi - \gamma_0)}, e^{j\zeta \cos(\phi - \gamma_1)}, \dots, e^{j\zeta \cos(\phi - \gamma_{M-1})}] \quad (2.12)$$

Equation 2.12 shows us that the phase shifting at each elements isn't linearly independent. The steering vector is not in Vandermonde structure like ULA steering vector.

The beam shape of the uniform circular array is periodic in azimuth angle. For this reason, it can be convert to different Fourier harmonics by using Fourier analysis (Davies, 1965). The phase mode excitation method is providing to convert the steering vector of incoming signal to Vandermonde structure.

Assume that we have a transformation matrix as T . Then, the incoming signal output, the array response and the noise signal can be determined like below,

$$\tilde{X}(t) = TX(t), \quad (2.13)$$

$$\tilde{A}(\phi) = TA(\phi), \quad (2.14)$$

$$\tilde{N}(t) = TN(t), \quad (2.15)$$

And then the output of impinging signal can be defined;

$$\tilde{X}(t) = \tilde{A}(\phi)S(t) + \tilde{N}(t) \quad (2.16)$$

Where the transformation matrix is;

$$T = JF \quad (2.17)$$

In the equation (2.18), J matrix and the resulting phase mode array beam pattern matrix F matrix can be denoted respectively as below,

$$J = \text{diag} \left\{ \frac{1}{\sqrt{M} j^m J_m(kr)} \right\}_{(2h+1) \times (2h+1)} \quad (2.18)$$

$$F = \frac{1}{\sqrt{M}} \begin{pmatrix} 1 & w^{-h} & w^{-2h} & w^{-3h} & \dots & w^{-(M-1)h} \\ \vdots & \vdots & \vdots & \vdots & \dots & \vdots \\ 1 & w^{-1} & w^{-2} & w^{-3} & \dots & w^{-(M-1)} \\ 1 & 1 & 1 & 1 & \dots & 1 \\ 1 & w^1 & w^2 & w^3 & \dots & w^{(M-1)} \\ \vdots & \vdots & \vdots & \vdots & \dots & \vdots \\ 1 & w^h & w^{2h} & w^{3h} & \dots & w^{(M-1)h} \end{pmatrix}_{(2h+1) \times M} \quad (2.19)$$

In Equation 2.18 and 2.19, $w = e^{\frac{j2\pi}{M}}$ is the phase-mode beamforming vector, $J_m(kr)$ denotes Bessel function of the first kind of the order depends on (kr) , $h \approx k_0 r$ is defined the maximum phase mode order and $m = (-h, \dots, 0, \dots, h)$ is represented phase range of beamforming vector.

There are two significant indispensable rules to apply phase mode excitation to UCA structure. The first significant rule is that Bessel function value is small when $|m| < kr$. In order to apply phase mode excitation to UCA structure with an acceptable highest mode. Therefore, the highest phase mode order must be $m \approx k_0 r \sin(\varnothing) \in [0, k_0 r]$.

The second one is about spatial Nyquist theorem. The number of the element in the UCA structure must be at least twice of the highest phase mode order.

As a result of these two major rules, the distance between two adjacent elements should meet $d \leq \lambda/2$ and the radius of the array must be $r_{max} = \frac{N\lambda}{4\pi}$.

The output of the steering matrix can be converted to VULA structure by

multiplying of the original array response matrix of the UCA structure with transformation matrix as in equation (2.14). Hereby, the converting array response matrix can be rewritten like below;

$$\tilde{a}(\varphi) = \begin{pmatrix} e^{-jh\varphi_1} & \dots & e^{-jh\varphi_p} \\ \vdots & \ddots & \vdots \\ e^{jh\varphi_1} & \dots & e^{jh\varphi_p} \end{pmatrix} \quad (2.20)$$

Afterward, the array manifold is in the Vandermonde structure. MUSIC techniques can be applied like ULA geometric form.

2.2.3 The Steering Matrix of L-Shaped Array

As it is depicted in Figure 2.4, an L-shaped array consists of two uniform linear array, which lied on the X and Y axes. The one of the antenna elements are common for two these ULA arrays.

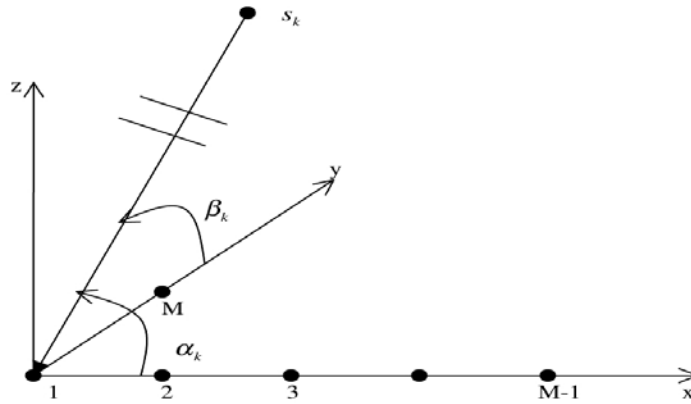


Figure 2.4 L-Shaped Array geometric structure (Xia & Du, 2006)

The distance between two adjacent elements is defined like the ULA array. The L-shaped array of the receiving signal of the steering matrix for each can be determined by using the ULA array equations. The array manifold for the ULA structure on X axes can be written as;

$$A_x(\varphi) = [a_x(\varphi_1), a_x(\varphi_2), \dots a_x(\varphi_K)] \quad (2.21)$$

Similarly, the array response for the ULA which it is on the Y axes can be defined;

$$A_y(\Phi) = [a_y(\Phi_1), a_y(\Phi_2), \dots, a_y(\Phi_K)] \quad (2.22)$$

where M , is the number of the elements in each array, K , is the number of the impinging signals on the array and d is the distance between two elements.

$$a_x(\Phi_K) = [a_{x,1}(\Phi_K), a_{x,2}(\Phi_K), \dots, a_{x,(M-1)}(\Phi_K)] \quad (2.23)$$

$$= [e^{j2\pi \cos(\Phi_K)d/\lambda}, \dots, e^{j2\pi (M-1)\cos(\Phi_K)d/\lambda}]^T \quad (2.24)$$

$$a_y(\Phi_K) = [a_{y,1}(\Phi_K), a_{y,2}(\Phi_K), \dots, a_{y,(M-1)}(\Phi_K)] \quad (2.25)$$

$$= [e^{j2\pi \sin(\Phi_K)d/\lambda}, \dots, e^{j2\pi (M-1)\sin(\Phi_K)d/\lambda}]^T \quad (2.26)$$

In order to obtain the main array manifold of the receiving signal, we will apply the property of kronecker products (Ma, Hsieh, & Chi, 2010).

$$A_{xy}(\Phi) = A_x(\Phi) \otimes A_y(\Phi) \quad (2.27)$$

2.3 Properties of Subspace DOA Methods

The subspace technique uses its approved properties that they are given below (Chen, Gokeda, & Yu, 2010);

- The eigenvectors spread out the spatial covariance matrix and include two subspaces; signal and noise subspaces and both of them are orthogonal.
- The steering vectors of the signal subspace.
- The smallest Eigen-values of covariance matrix is spanned the noise subspace.
- The biggest Eigen-values of covariance matrix is spanned the signal subspace.

2.3.1 Multiple Signal Classification Method

Multiple Signal Classification methods is one of the most popular of the DOA technique. It has a high resolution and low-computation complexity (Pal &

Vaidyanathan, 2010). Also, it overcomes the fundamental limitations of methods such as the Bartlett and Capon (Ioannides & Balanis, 2005).

The MUSIC algorithm is a subspace-based method that used the array output signal of covariance matrix to estimate parameters of multiple signals. In MUSIC algorithm, it is accepted that the covariance matrix of the noise has uniform power on the diagonal as $W_n = \sigma^2 I$, where I is the identity matrix. The covariance matrix of the array output signal can be determined as:

$$R = [\tilde{X}\tilde{X}^H] = AR_sA^H + \sigma^2 I \quad (2.28)$$

It assumes that the number of the source signals are known and not correlated. Also it accepted that the estimate signal covariance matrix has a full rank. In Equation 2.28; R_s is denoted covariance matrix, A is array manifold, A^H , Hermitian matrix of the array manifold and $\sigma^2 I$ is the noise covariance matrix.

The Eigen decomposition will be provided to obtain the eigenvalues and eigenvectors of the covariance matrix. The eigenvalues are

$$\{\lambda_1 \geq \lambda_2 \geq \dots \geq \lambda_M\} \quad (2.29)$$

and the eigenvectors are

$$\{v_1, v_2, \dots, v_M\} \quad (2.30)$$

The MUSIC can provide number of incoming signals, direction of arrival, the power of incoming signals, noise signal power and correlation of the signals. The number of impinging signals are determined by using the Eigen values. The number of Eigen values of covariance matrix which is not equal to zero will give the number of incoming signals.

The Eigen vectors of R covariance matrix are using to obtain the direction of arrival of the receiving signals. The noise subspace is orthogonal to the array response vector as in equation 2.31.

$$\{v_{p+1}, v_2, \dots, v_M\} \perp \{\tilde{\alpha}(\phi_1), \tilde{\alpha}(\phi_1), \dots, \tilde{\alpha}(\phi_p)\} \quad (2.31)$$

The spatial spectrum of the MUSIC can be given as;

$$P_{MUSIC}(\phi) = \frac{1}{\sum_{i=p+1}^M |\tilde{\alpha}^H|^2}, \quad \tilde{\alpha}^H v_i = 0, \quad i = p + 1, \dots, M \quad (2.32)$$

The MUSIC spectrum will occur at the direction of the arrival estimation of the receiving signal. And DOA estimation can obtain to utilize these peaks.



CHAPTER THREE

METHODOLOGY

In this chapter, firstly we will explain to implementation of algorithms with ULA, UCA, and L-Shaped array geometric configurations. After that, we will synthesize three geometric configurations by their error weight function and try to optimize results for getting better DOA estimations.

3.1 Implementation of MUSIC Algorithm for ULA Configuration

As it can be seen in Figure 3.1, ULA array has two antennas. There are 45-degree angle between array line and X axes. Because of the ULA has symmetrical structure, we will assume that there are no angle differences between array line and X axes. We will apply MUSIC algorithm. After determining the DOA, we will add 45 degrees to result of DOA.

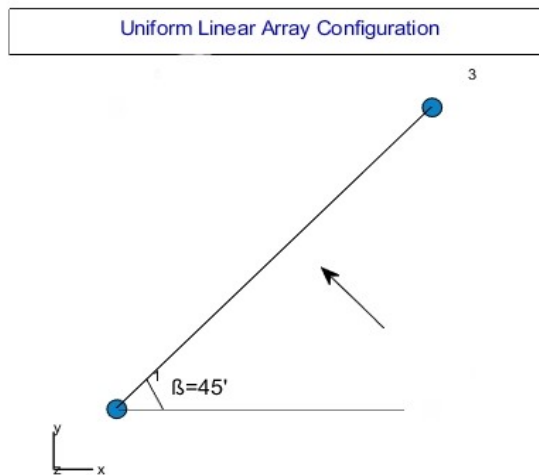


Figure 3.1 Uniform linear array configuration which consist two elements

The distance between two adjacent elements is $\leq \frac{\lambda}{2}$, the frequency of the signal is 2.45 GHz. The distance can be calculated by using Equation 2.6. Therefore, the ULA structure just have two number of elements, it can be estimated only single source of incoming signal.

As the ULA has two number elements, the array manifold of incoming signal can be determined;

$$A(\varnothing) = [\alpha_1(\Phi_1)]_{2 \times K} \quad (3.1)$$

And the output of the incoming signal vector is;

$$X(t) = \alpha(\varnothing)S(t) + N(t) \quad (3.2)$$

For the above equation, the size of X and the additive white noise signal vector N is $(2 \times K)$, which K represent the number of snapshot of the incoming signal. The size of the incoming signal (S), is $(1 \times K)$. The flow chart of the DOA estimation algorithm, for ULA structure can be expressed step by step like in Figure 3.2.

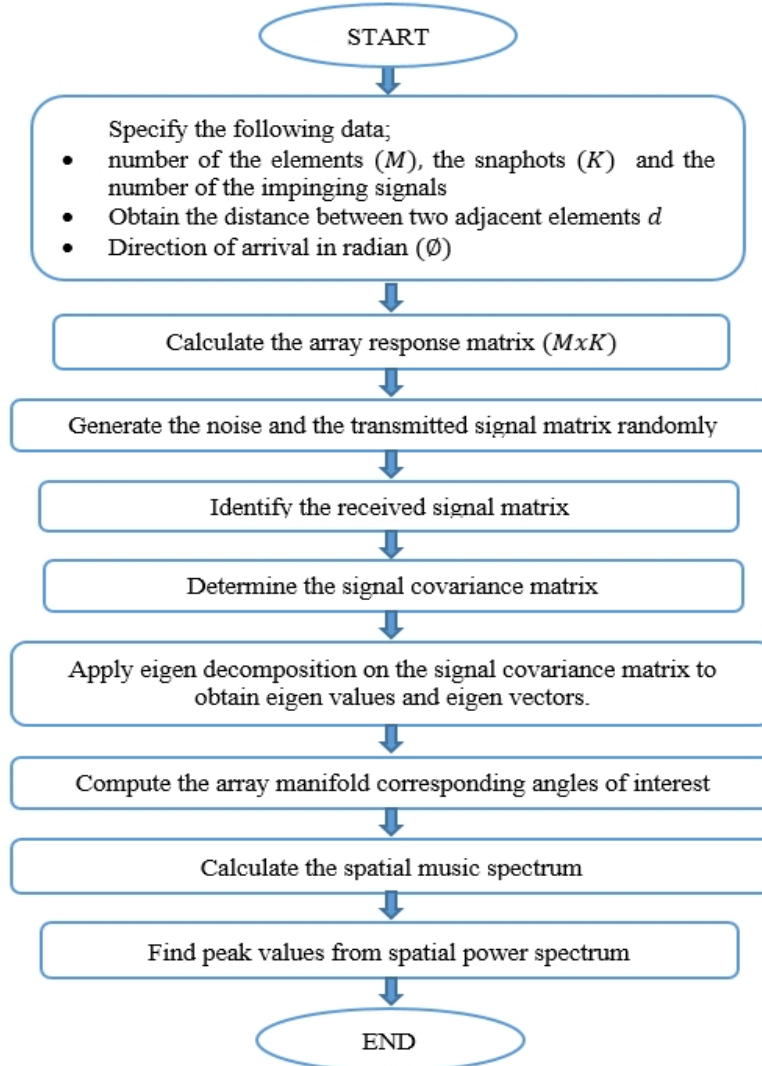


Figure 3.2 The flow chart of the DOA estimation for ULA structure

3.2 Implementation of MUSIC Algorithm for the ULSA Configuration

The ULSA geometric configuration for our implementation can be seen in Figure 3.2 In our constructions we have only two antenna elements in each X and Y axes arrays. The distance between two adjacent elements is $d_{ULA}/\sqrt{2}$.

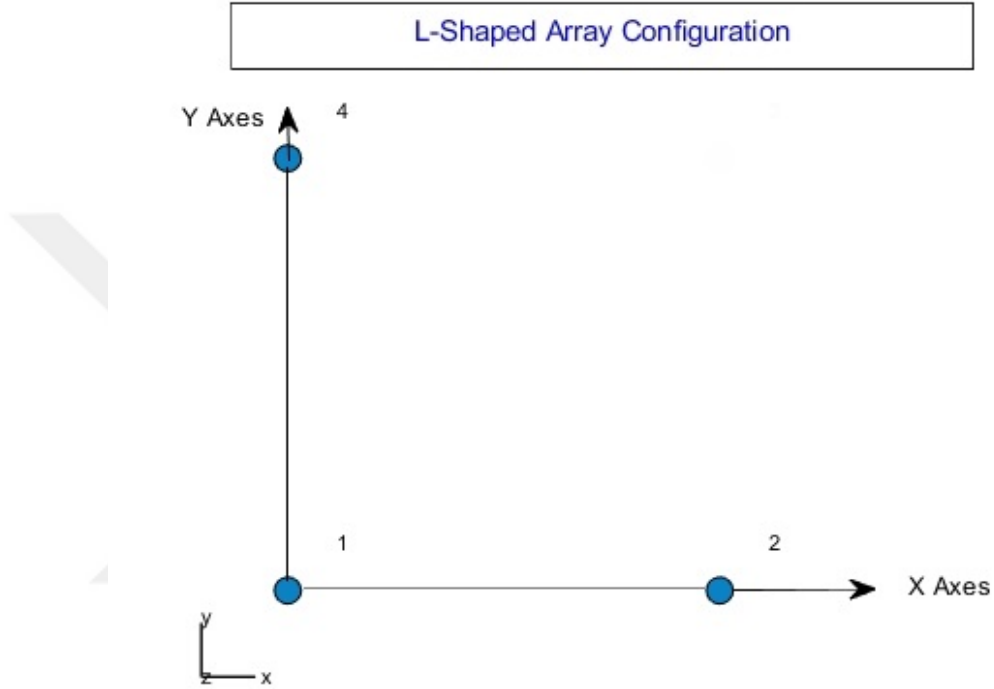


Figure 3.3 The ULSA geometric structure in our implementation

The array manifold of the ULSA structure can be determined as below;

$$a_x(\phi_k) = [a_{x,1}(\phi_k), a_{x,2}(\phi_k)] \quad (3.3)$$

$$= [1, e^{j2\pi \cos(\phi_k)d/\lambda}]^T \quad (3.4)$$

$$a_y(\phi_1) = [a_{y,0}(\phi_1), a_{y,1}(\phi_2)] \quad (3.5)$$

$$= [1, e^{j2\pi \sin(\phi_k)d/\lambda}]^T \quad (3.6)$$

Then the results of the main steering array of the matrix can be written as;

$$a_{xy}(\phi_1) = [a_x(\phi_1) \otimes a_y(\phi_1)]_{4 \times 1} \quad (3.7)$$

Then the MUSIC algorithm can be directly applied to obtain the direction of the arrival estimation.

3.3 Applying MUSIC Algorithm to UCA Configuration

The UCA geometric structure which is used in this thesis is depicted in Figure 3.3 and as it can be seen the configuration has four elements. In this dissertation, we are just interested one dimensional of the DOA estimation. Because of that the elevation angle was taken 90° .

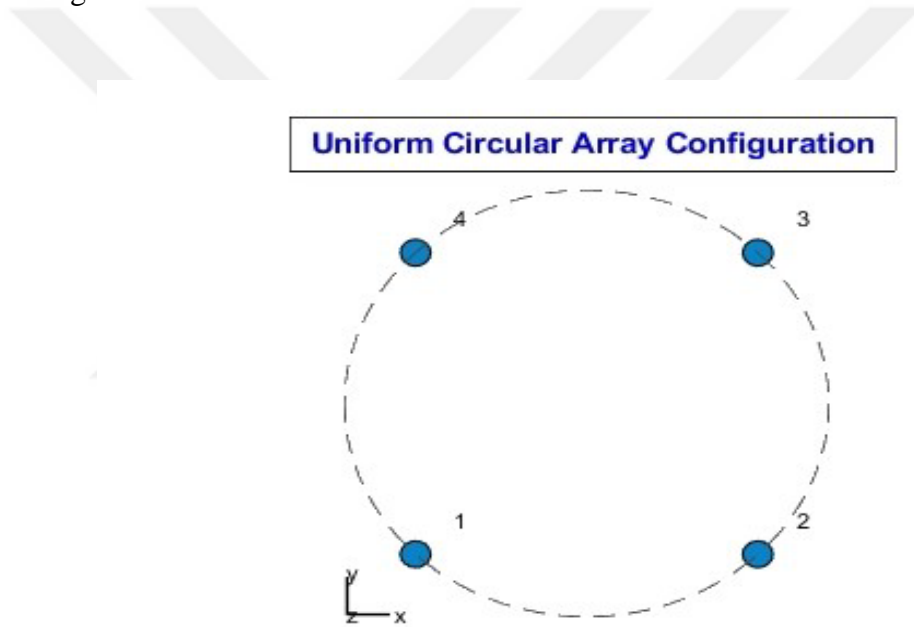


Figure 3.4 Uniform circular array configuration with four elements

The array response of the UCA structure can be determined in Equation (2.11). As it was expressed in section 2.2.2; if it is taken elevation angle as 90° , then $\zeta = k_0 r$ and $\gamma_n = \frac{\pi(n-1)}{2}$. By using these two definitions, the steering vector can be calculated as,

$$\alpha(\phi) = [e^{j\zeta \cos(\phi-\gamma_0)}, e^{j\zeta \cos(\phi-\gamma_1)}, e^{j\zeta \cos(\phi-\gamma_2)}, e^{j\zeta \cos(\phi-\gamma_3)}] \quad (3.8)$$

First of all, the highest phase mode order of the Bessel function must be determining to calculate the phase mode beamforming vector. The highest phase mode was determined by $m \approx k_0 r \sin(\varnothing) \in [0, k_0 r]$, when $\varnothing = 90^\circ$.

Afterward, the phase beamforming vector and the resulting phase mode array beam pattern matrix can be written as below respectively, where the $w = e^{\frac{j2\pi}{M}}$, $M = 4$ and $m = 2$.

$$J = \text{diag} \left\{ \frac{1}{\sqrt{M} j^m J_m(kr)} \right\}_{(5) \times (5)} \quad (3.9)$$

$$F = \frac{1}{\sqrt{M}} \begin{pmatrix} 1 & w^{-2} & w^{-4} & w^{-6} \\ 1 & w^{-1} & w^{-2} & w^{-3} \\ 1 & 1 & 1 & 1 \\ 1 & w^1 & w^2 & w^3 \\ 1 & w^2 & w^4 & w^6 \end{pmatrix} \quad (3.10)$$

Then, the transformation matrix can be figure out by multiplying J and F matrix. As it is defined in equation (2.14), the UCA steering vector of the VULA version can be figure out as below;

$$\tilde{\alpha}(\varnothing) = \begin{pmatrix} e^{-j2\varnothing_1} \\ e^{-j\varnothing_1} \\ 1 \\ e^{j\varnothing_1} \\ e^{j2\varnothing_1} \end{pmatrix} \quad (3.11)$$

Now, we can determine the output of the incoming signal matrix,

$$\tilde{X}(t) = \tilde{\alpha}(\varnothing)S(t) + \tilde{N}(t) \quad (3.12)$$

Finally, it can be performed MUSIC algorithm to obtain the DOA estimation, as it is a ULA form. The flow chart of the DOA estimation for UCA-MUSIC can be expressed like below;

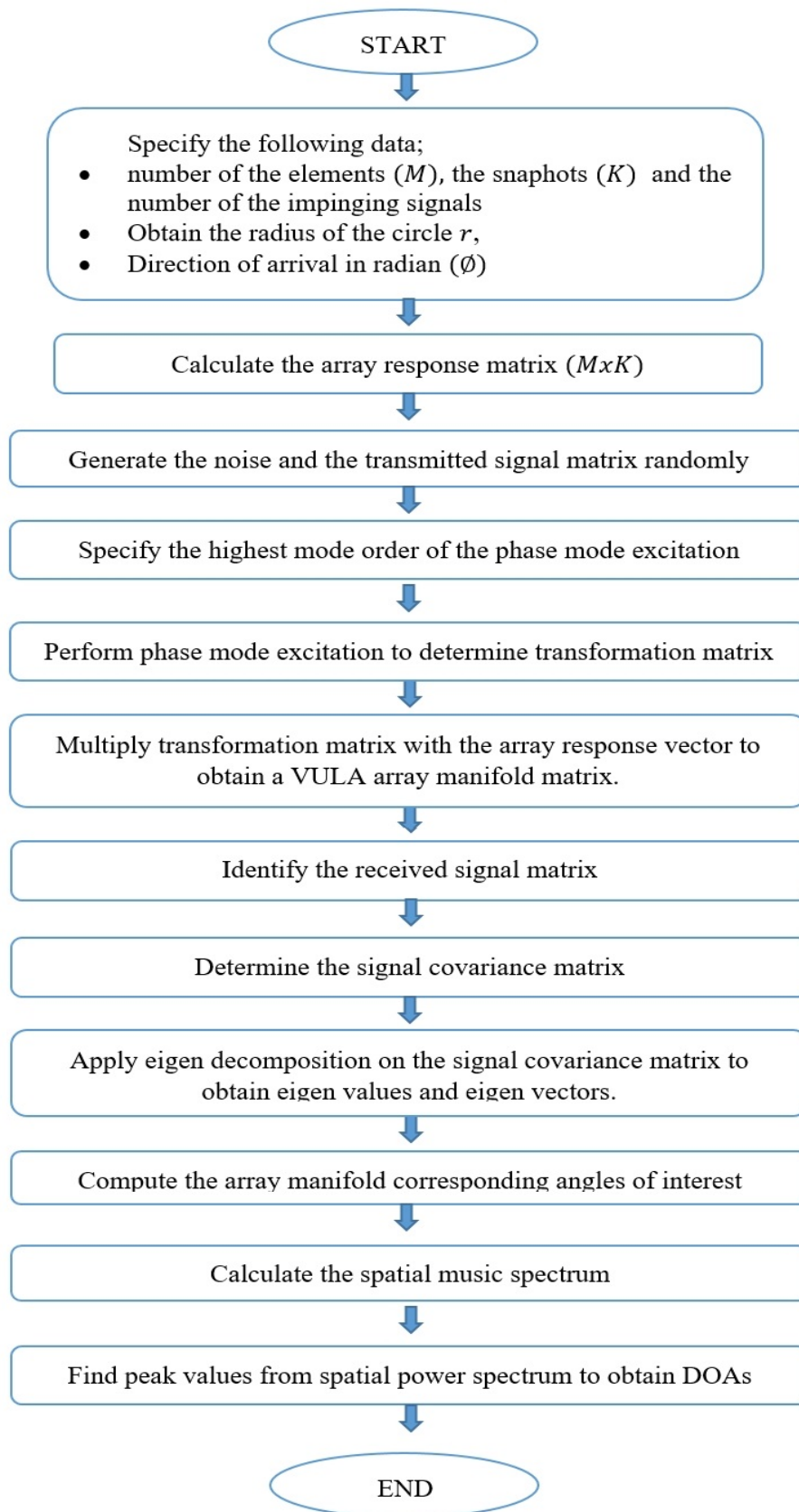


Figure 3.5 The flow chart of the DOA estimation for UCA structure

3.4 Determining DOA by Applying Multiple Algorithm via Their Error Weight Function

In order to evaluate the results of the DOA estimations for all geometric structures, the angle ranges of the all configurations must be put on the same angle scale. Thus, it has widest azimuthally coverage, we choose the UCA configuration as reference. In figure 3.4, It can be seen that we start the reference point from the first antenna element of the UCA. When we get this point as a reference the scale of angles for all configurations will be like below;

- The ranges of the UCA is between 0° to 360° .
- The coverage of the ULA will be 135° to 305° .
- The ULSA angle range will be 180° to 270° .

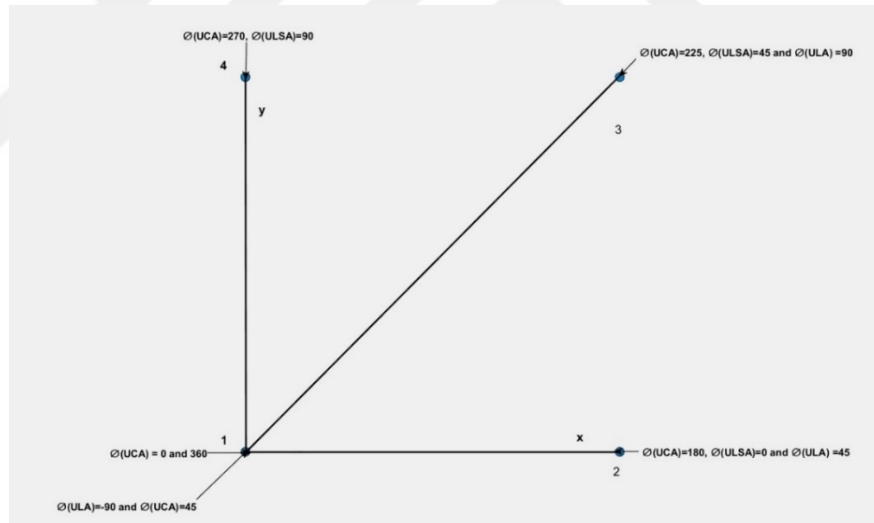


Figure 3.6 Put on all the DOA configurations in same scale

In order to combine all the DOA results together, we perform the MUSIC algorithm to the geometric structure on their own scale, then we shift the results to the common scale. To convert the ULA and the ULSA structure angles of the receiving signal as the UCA scale, the equations (3.14) and (3.15) can be used respectively.

$$\Phi_{Common} = \Phi_{UCA} \quad (3.13)$$

$$\phi_{Common} = \phi_{ULA} + 135^\circ \quad (3.14)$$

$$\phi_{Common} = \phi_{ULSA} + 180^\circ \quad (3.15)$$

Afterwards, the results of the DOA estimations can be compared easily. In order to combine and increase the accuracy of the DOA results, Equation 3.16 is used. It is chosen the best configuration to achieve higher performance values.

$$DOA = \begin{cases} \text{if, } \phi_{Common} = 0^\circ \text{ to } 145^\circ \text{ and } 145^\circ \text{ to } 295^\circ, DOA = \phi_{UCA} \\ \text{if, } \phi_{Common} = 145^\circ \text{ to } 295^\circ, DOA = \min(\phi_{UCA}, \phi_{ULA}) \\ \text{if, } \phi_{Common} = 190^\circ \text{ to } 260^\circ, DOA = \min(\phi_{UCA}, \phi_{ULSA}, \phi_{ULA}) \end{cases} \quad (3.16)$$

CHAPTER FOUR

RESULTS

In order to analyze the performance of the configurations, we have made several simulations. The classical MUSIC algorithm was applied to three array structures. In these section, we will show the simulation results for ULA, UCA and ULSA geometric configurations respectively. Then, we will simulate for specific angle ranges to compare the performance of the structures. Finally, the results of DOA estimations will be combined for two or three configurations to increase the performance for blind range angles which it is the main aim of this study.

There are several parameters which effect the results of the DOA estimations performance like; SNR, number of the trials and snapshots, and the value of the receiving signal. We will make simulation to observe the effect these parameters.

4.1 Simulation Result of ULA Configuration

The first simulation was made for the ULA configuration. There is right proportion between the DOA estimation and SNR. The relationship of the DOA estimation and the SNR can be seen in Figure 4.1. As it is expected, when the SNR value is 0, the error value is about 6 degrees, and when the SNR value is 16, the error value is under 1 degree.

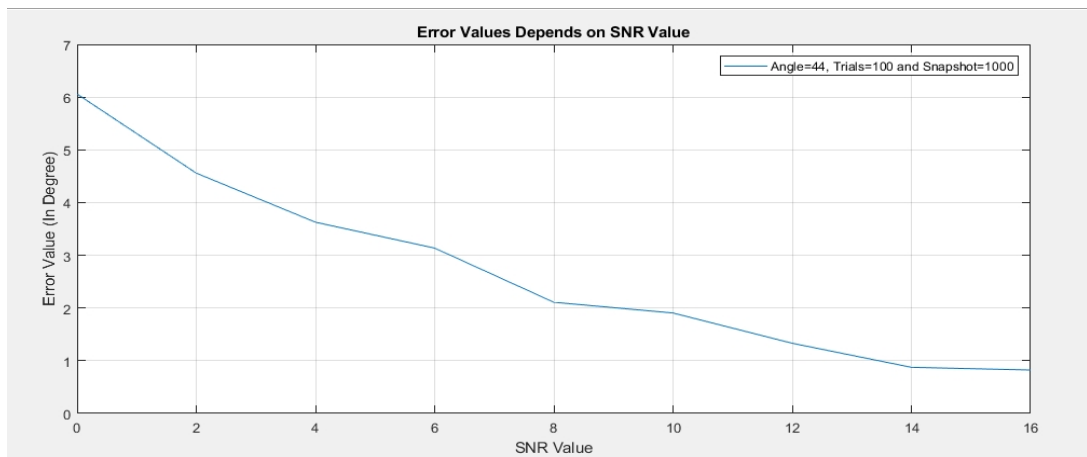


Figure 4.1 Simulation for $\theta=44$, Trials=100, Snapshots=1000 and SNR=0 to 16

As previously mentioned, the results of the DOA estimations are varying by the incoming of the signal angle. The angle range of the DOA estimation is chosen generally between -90 to 90 degree. However, the ULA configurations has a suffer, when the angle values are between the -90 to -85 and 85 to 90 degree. Thus, our ULA structure has only two number of the elements, we have range for the DOA estimations. The performance of the DOA estimations for the angles between -70 to 70 degree is presented in Figure 4.2. By increasing the SNR and the number of the snapshots, the results can be taken for wider range. But the computation time will rise dramatically.

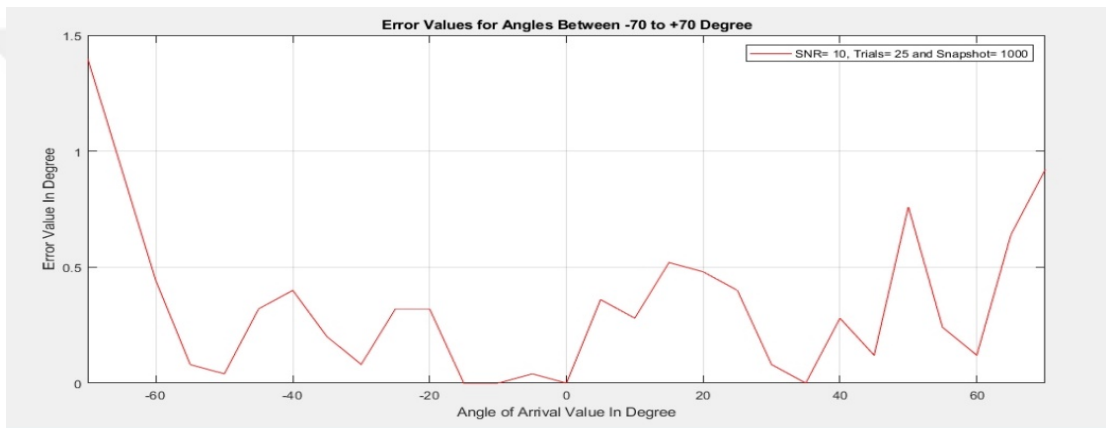


Figure 4.2 Trials = 25, Snapshots=1000, SNR=20, DOA=-70 to 70 Degree

The peaks of the spatial MUSIC spectrum are used to determine the DOA estimations. In the Figure 4.3, it can be seen that the peaks cannot occur properly, when the angle of the incoming signal is -85 degree.

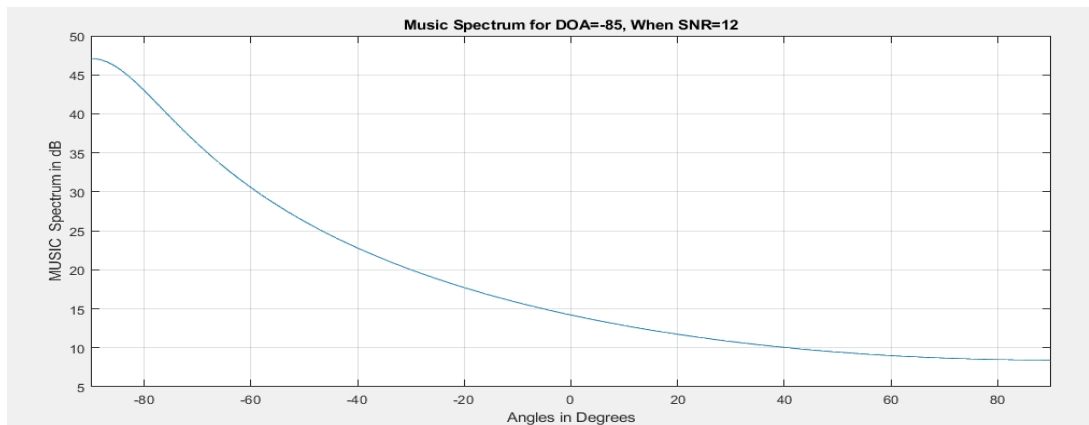


Figure 4.3 The Spatial Music Spectrum When the DOA=-85

4.2 Simulation Result of ULSA Configuration

The L-Shaped Array configuration is very similar to the ULA geometric structure. It consists two ULA configuration. As the ULA construction, it has some angle ranges to handle the DOA estimations. The accuracy of the estimation is better than the ULA configuration. In Figure 4.4, the error of the estimations by varying to SNR is depicted.



Figure 4.4 The Relation of the SNR and the error estimation of the ULSA structure

The one of the most significant disadvantages of the ULSA configuration is the azimuthally coverage angle. However, it can cover only 90 degrees, the configuration has very poor performance in some ranges. The error values of the estimations can be seen in Figure 4.5, while the angle of the incoming signals are between 10° to 80°.

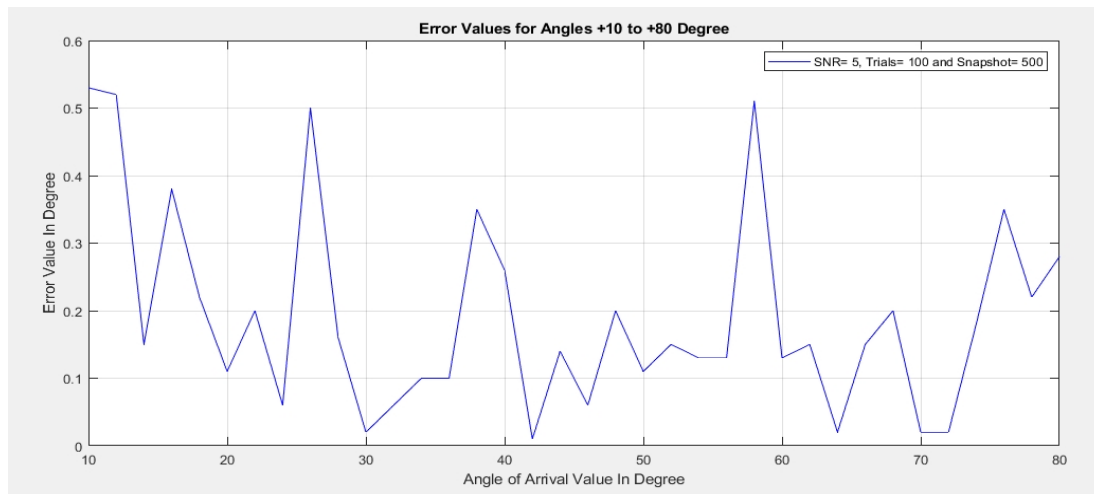


Figure 4.5 The DOA estimations for the ULSA structure (DOA =10o-80o)

When the direction of the arrival angle is between 0° to 10° and 80° to 90° , the accuracy of the DOA estimations is very low. Most of the time, it cannot handle to determine the angle of the receiving signal. In Figure 4.6, the spatial power of the MUSIC spectrum can be viewed, when the direction of the arrival angle equals 7° . The peak cannot occur properly, so the DOA estimation cannot be determined.

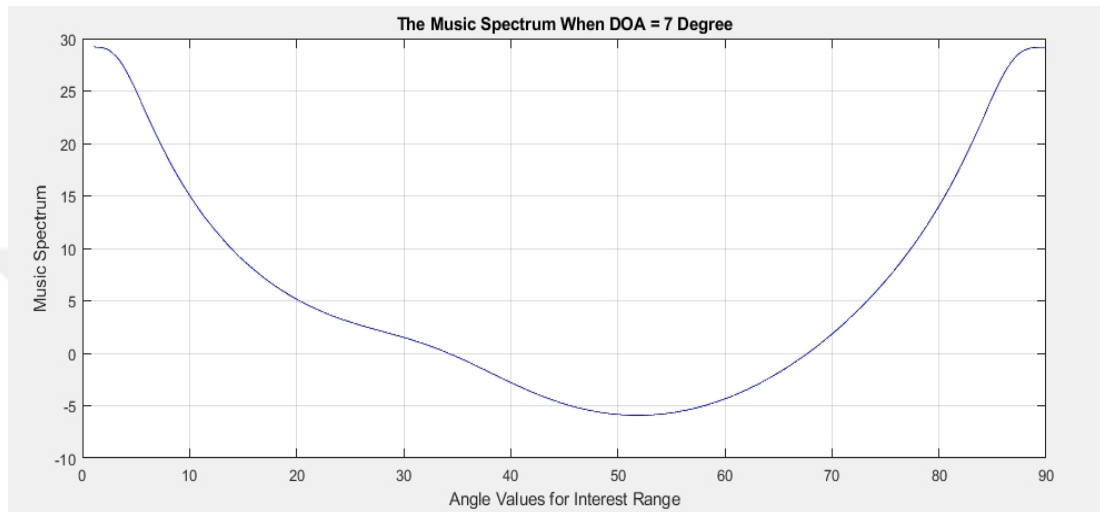


Figure 4.6 The spatial MUSIC spectrum of the ULSA when DOA= 7°

4.3 Simulation Result of UCA Configuration

The UCA configuration has some advantages when we compare with the ULA and ULSA structures. It can azimuthally cover between 0 and 360 degrees. Moreover, it can handle to estimate multiple incoming signals simultaneously. As we have only 4 number of the elements, the UCA configuration can obtain two angle of the receiving signals in our configuration. We have been made simulations by varying the parameters for single and two source impinging signal respectively.

4.3.1 Simulation Results of the UCA Structure for Single Source Receiving Signal

The relationship between the SNR and the performance of the DOA estimation is like the ULA configuration. The results of the UCA structure are better than the ULA configuration, as it can be seen in the below figure. The UCA structure has very good results even when the SNR is low.

The accuracy of the DOA estimations for the uniform circular array geometric structure is poor for some angles, as we can see some results for the ULA configuration. The UCA structure can handle to obtain the DOA estimations, but the error value is very high. In Figure 4.7, it can be seen the relationship between the DOA estimation performance with SNR values.

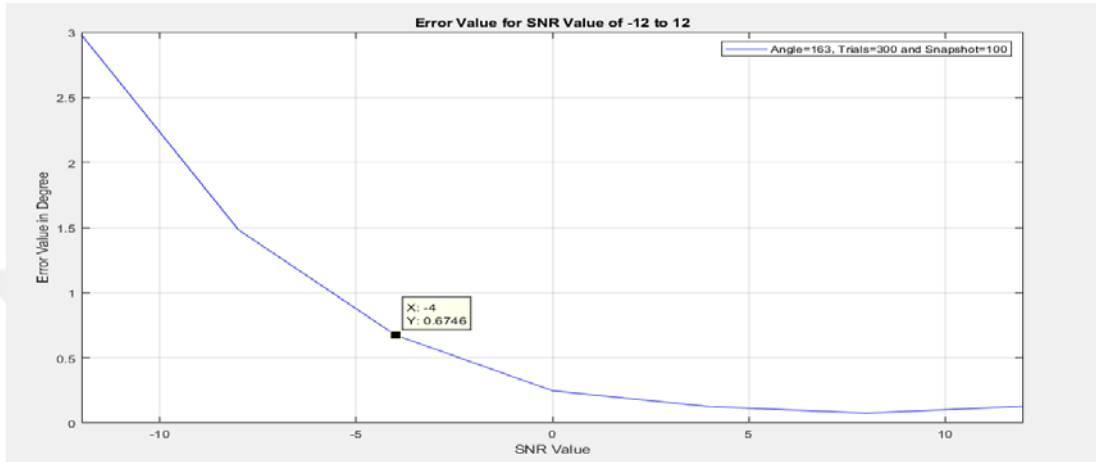


Figure 4.7 The Performance of the UCA structure When SNR is between -12 to 12

In Figure 4.8, It can be seen which the angle values are changing between 10 to 350 degree. The DOA estimations for that range is very successful.

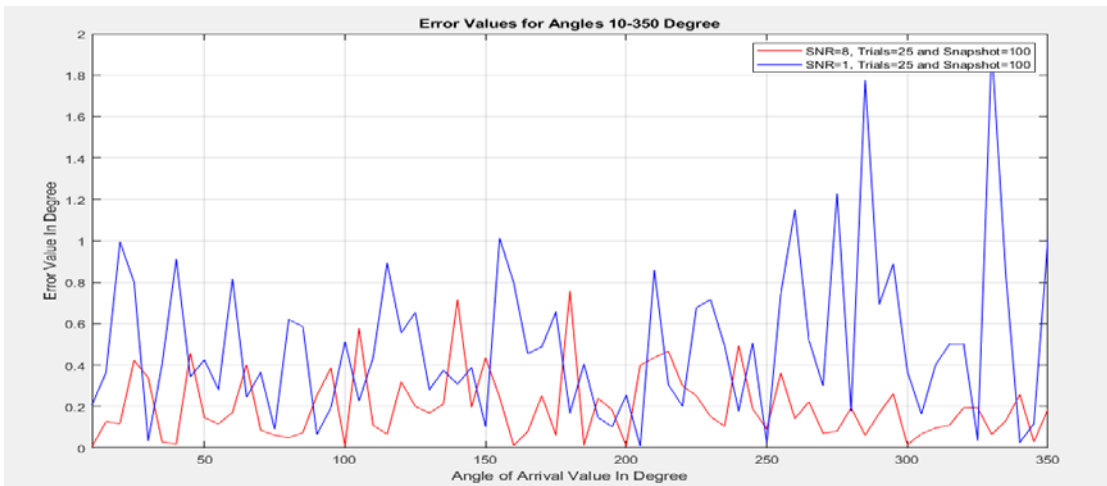


Figure 4.8 The Error values of the DOA estimations When DOA=10-350

The simulation is performed for all efficient angle ranges with two different SNR value. As it is expected, when the SNR value is high the error values are low and when the SNR value is low, the error values are high.

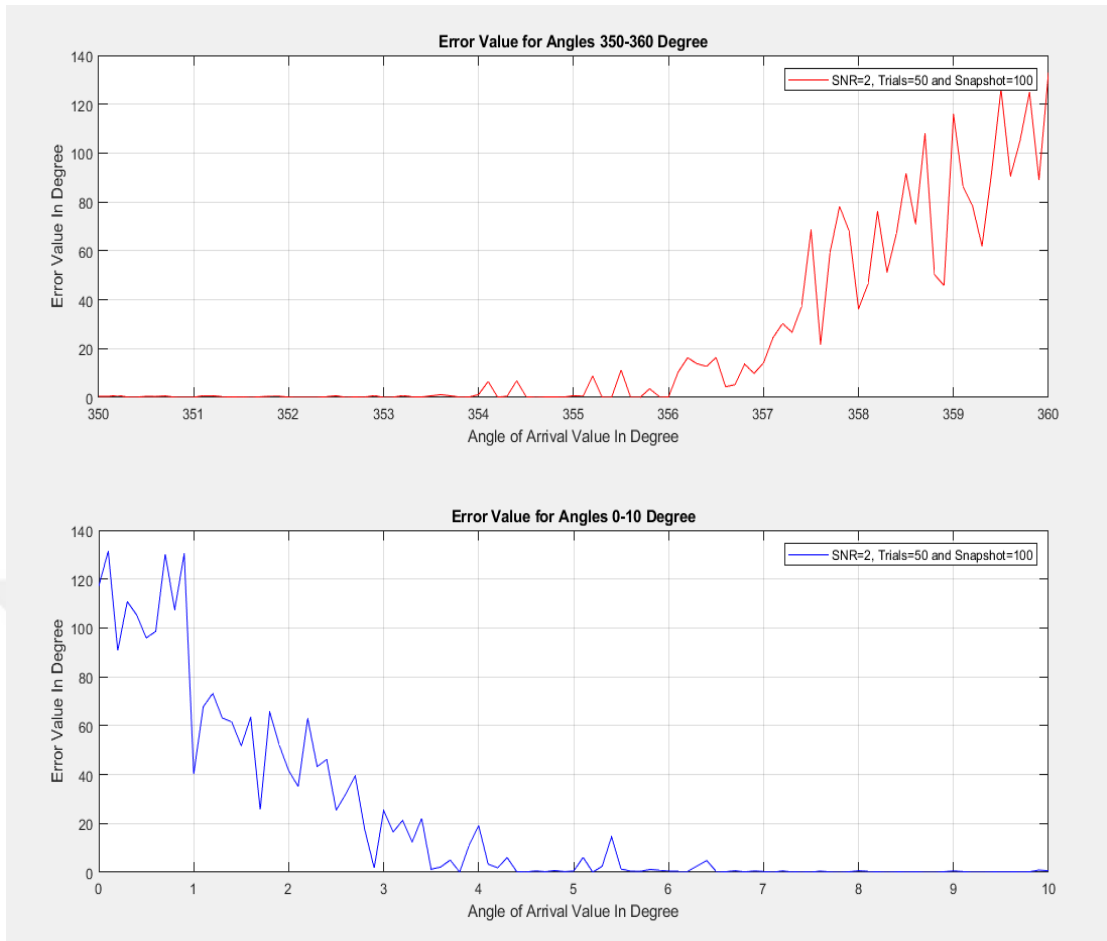


Figure 4.9 The error value of the estimations, when $\phi=350-360$ and $\phi=0-10$ degree

The UCA structure cannot handle to estimate some of the incoming angles. The results of the estimations for angles between 0-10 and 350-360 degrees can be seen in Figure 4.9. As it is presented in figure, the accuracy of the DOA estimation is very low, and it is not efficient for determining the angle of the receiving signal.

4.3.2 Simulation Results of the UCA Structure for Two Source Receiving Signal

Because of the ULA and ULSA hasn't enough number of the elements, the UCA is the only structure to estimate two number of the receiving of signals simultaneously, in our implementations. Therefore, we have just the four number of the antenna elements in the UCA configuration, the angle values of between two incoming signal source must be high to obtain the DOA estimations. The spatial power of the MUSIC

spectrum can be seen in Figure 4.10, when $\phi_1=163$ and $\phi_2=233$, the number of the trials=100 and the number of the snapshots is 200.

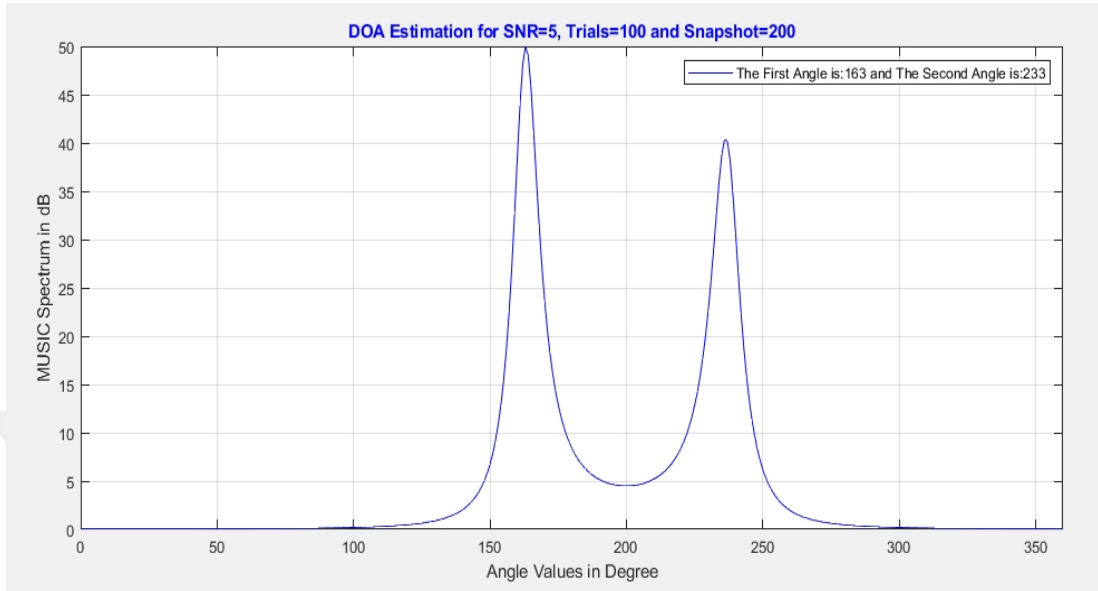


Figure 4.10 The MUSIC spectrum for two impinging signals with high resolution

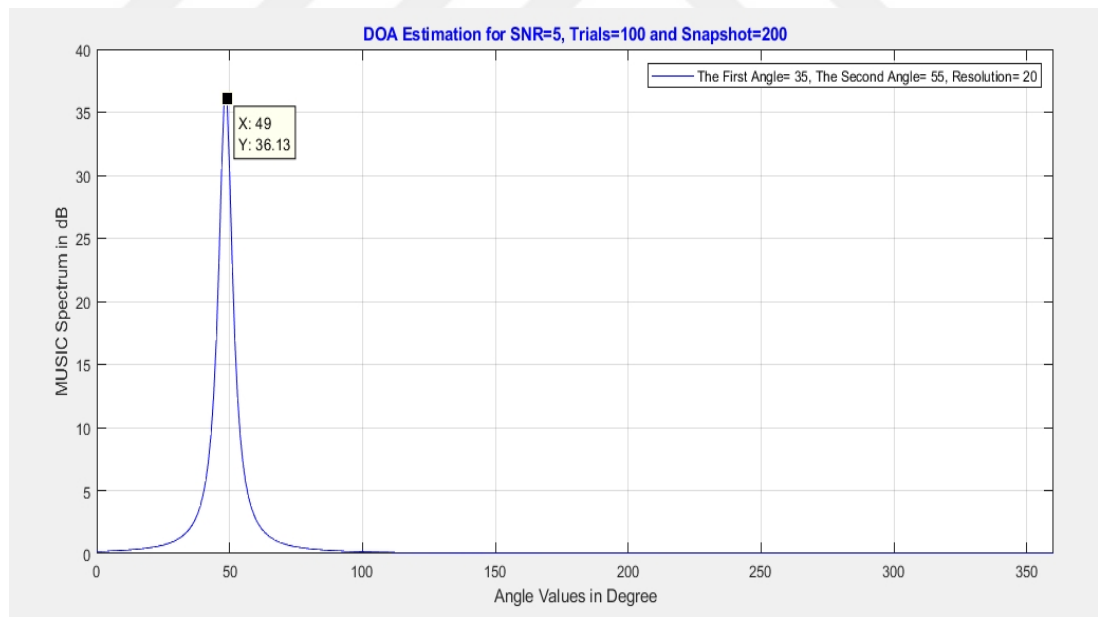


Figure 4.11 The MUSIC spectrum for two impinging signals with low resolution

The resolution is defined the difference between two angles of the receiving signal. When the resolution is low, only one peak occurs on the spatial power of the MUSIC spectrum and the positions of the peak is between two angles as it can be seen in Figure

4.11. That's why, only one of the DOA estimations can be obtained. Generally, the result of the DOA estimation value is the average of the two incoming angles, when the resolution is low.

Table 4.1 The Result of 2 DOA Estimation for UCA Configuration

Angle of the 1st incoming signal	DOA estimation of the 1st incoming signal	Error for the 1st DOA (Degree)	Angle of the 2nd incoming signal	DOA estimation of the 1st incoming signal	Error for 2nd DOA (Degree)	Explanation
20	-	-	35	-	-	SNR=0, Snapshot=2000
20	27.36	7.36	35	301.52	266.52	SNR=0, Snapshot=20000
20	23.17	3.17	35	115.21	80.21	SNR=6, Snapshot=20000
20	20.55	0.55	35	34.56	0.44	SNR=10, Snapshot=20000
20	21.70	1.70	40	55.05	15.05	SNR=10, Snapshot=2000
20	20.40	0.40	45	44.42	0.58	SNR=10, Snapshot=2000
20	21.96	1.96	50	61.63	11.63	SNR=5, Snapshot=2000
20	20.68	0.68	55	53.90	2.10	SNR=5, Snapshot=2000
20	21.05	1.05	55	53.60	2.40	SNR=5, Snapshot=1000
20	22.61	2.61	60	68.73	8.73	SNR=5, Snapshot=500
20	20.89	0.89	70	69.85	0.15	SNR=5, Snapshot=500
20	21.63	1.63	70	68.40	1.60	SNR=5, Snapshot=250
20	20	0	120	119.92	0.08	SNR=5, Snapshot=250

The DOA estimations of the results for two incoming signals with different incoming angles and by varying other parameters can be seen in Table. The following results can be drawn from table;

- The number of the snapshots has a significant impact on the DOA estimations. When the number of the snapshots is high, it can handle to determine two incoming signals of the angle, even when the resolution is low.
- In order to increase the accuracy of the DOA estimations SNR and the number of the snapshots should be raised, when the resolution is low. The histogram

of the estimations for the first angle of the receiving signal is 20 degrees and the second angle of the incoming signal is 35 in depicted in Figure 4.12. However, when the number of the snapshots is increased by two times, the computation time is raising more than two times.

- The error of the DOA estimations is low, while the resolution is higher than 40 degrees.

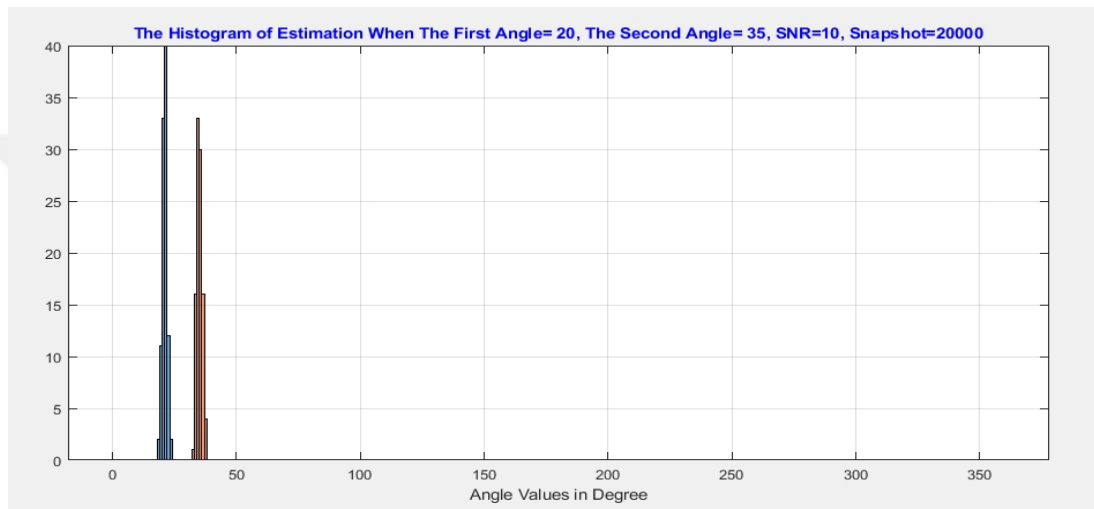


Figure 4.12 The histogram of the estimations when SNR=10 the snapshots=20000

4.4 Comparing ULA, ULSA and UCA structures

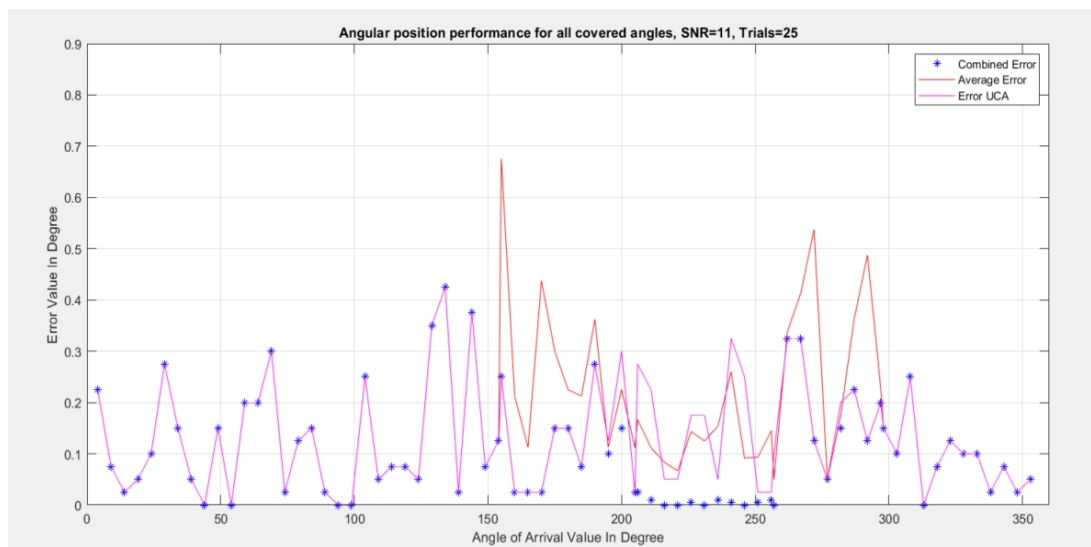


Figure 4.13 Comparing the DOA estimations for Combined Error, Average Error and UCA

The performance of the angular position is depicted in Figure 4.13. It is clear that the combined error value is equal or lower than UCA geometrical structure. So, the combined DOA estimation algorithm has better performance than UCA.

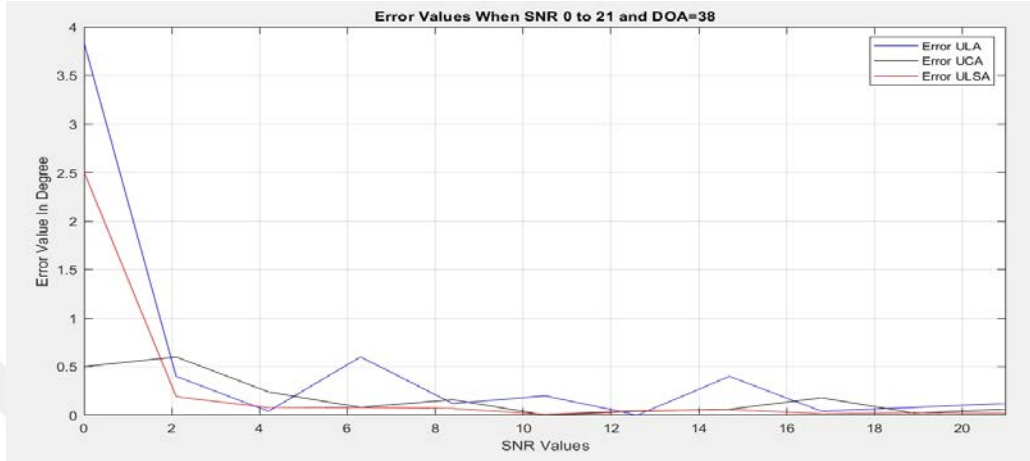


Figure 4.14 Comparing the performance of the ULA, ULSA, UCA by SNR

In Figure 4.14, it is presented the error values, when the SNR value is between 0 to 21. This figure shows us the overall performance of UCA structure is better than other structures, when the SNR value is low.

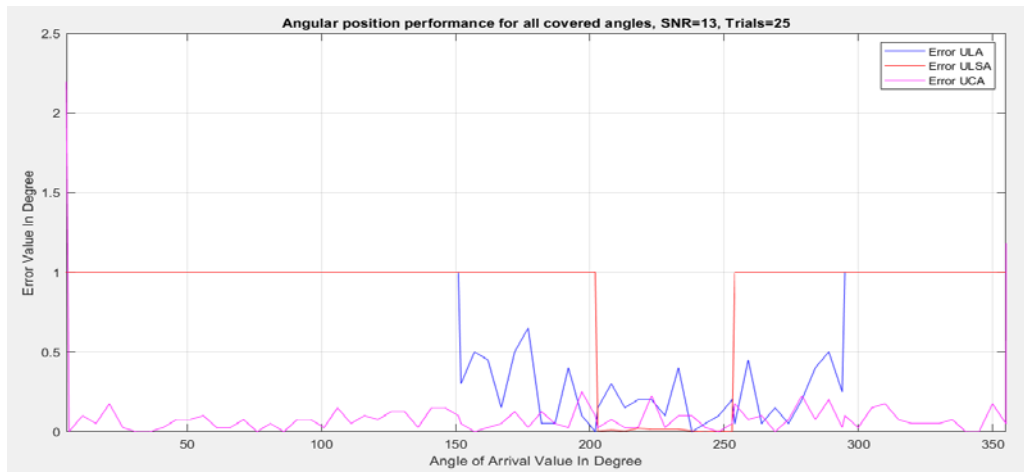


Figure 4.15 Comparing the performance of the ULA, ULSA, UCA by angle

The result of the DOA estimations error for angles between 3 to 356 degrees is presented in Figure 4.15. The error of DOA estimations is taken as 1 degree, for ULA and ULSA, when the angles are not covered by them. The performance of the DOA estimation is low for all structures, when the angles are at the beginning or at the end of the coverage angle range.

CHAPTER FIVE

CONCLUSION

In this dissertation, we represent a 1-D direction of arrival estimation solutions with several antenna array configurations by performing MUSIC subspace method. We have an UCA array with four antenna elements. We compose three different array configurations, by using the antenna position variations.

The first array structure is the uniform circular array, which it includes all four antenna elements and can cover 360° azimuthally. The results of the DOA estimations for the single incoming signal are very good, when the SNR is over 2, and the angle of the receiving signal is between 5° to 355° . However, while the number of the incoming signals is more than one, the UCA configuration cannot handle to obtain the DOA estimation for low resolution. In order to get better estimations for two incoming signal sources, the number of the signal snapshots must be increased. However, when the number of the snapshots increase, the computation load is rising.

The second array structure is the uniform linear array, which it has only two antenna elements. The ULA configuration can able to cover 180° azimuthally. Thus, it consists only two elements, it can handle to obtain the DOA estimations for only single source signal.

The third array structure is the L-shaped array, which it includes two ULA configurations that has two antenna elements. As the ULA configuration, the ULSA can be used to obtain the angle of the single signal source. The azimuthally angle coverage limit is worse than the ULA and the UCA. However, the accuracy of the DOA estimations is better than the ULA and the UCA configurations, when the receiving angle of the signal is in its range.

Finally, we combine the DOA estimations for all array structure to improve the accuracy of the DOA estimations. We get the better estimations, when the angle of the incoming signals is between common angle of two or three structures.

REFERENCES

- Al Jabr, K., Kwon, H. M., & Tayem, N. (2008). Modified UCA-ESPRIT for estimating DOA of coherent signals using one snapshot. In *Vehicular Technology Conference, 2008. VTC Spring 2008*. 290-293. IEEE.
- Balanis, C. A., & Ioannides, P. I. (2007). Introduction to smart antennas. *Synthesis Lectures on Antennas*, 2(1), 1-175.
- Bartlett, M. S. (1950). Periodogram analysis and continuous spectra. *Biometrika*, 37(1/2), 1-16.
- Borenstein, J., & Feng, L. (1994). *UMBmark: A method for measuring, comparing, and correcting dead-reckoning errors in mobile robots*. Technical report #94-22.
- Borenstein, J., Everett, H. R., & Feng, L. (1996). *Navigating mobile robots: Systems and techniques*. Wellesley, MA: AK Peters.
- Burg, J. P. (1967). *Maximum entropy spectral analysis*. In *37th Annual International Meeting, Soc. of Explor. Geophys.*, Oklahoma City
- Camps, A., Cardama, A., & Infantes, D. (2001). Synthesis of large low-redundancy linear arrays. *IEEE Transactions on Antennas and Propagation*, 49(12), 1881-1883.
- Capon, J. (1969). High-resolution frequency-wavenumber spectrum analysis. *Proceedings of the IEEE*, 57(8), 1408-1418.
- Chan, A. Y. J., & Litva, J. (1995). MUSIC and maximum likelihood techniques on two-dimensional DOA estimation with uniform circular array. *IEE Proceedings-Radar, Sonar and Navigation*, 142(3), 105-114.

- Chen, Z., Gokeda, G., & Yu, Y. (2010). *Introduction to Direction-of-arrival Estimation*. Norwood: Artech House.
- Cisco (2008). Wi-Fi Location-Based Services 4.1 Design Guide. American Headquarters, Cisco Systems Inc., USA.
- Cox, I. J. (1990). Blanche: Position estimation for an autonomous robot vehicle. In *Autonomous robot vehicles*, 221-228. New York, NY., Springer.
- Davies, D. E. N. (1965). A transformation between the phasing techniques required for linear and circular aerial arrays. In *Proceedings of the Institution of Electrical Engineers 112(11)*, 2041-2045. IET Digital Library.
- Davies, D. E. N. (1983), "Circular arrays," in Rudge et al. (eds): *The Handbook of Antenna Design (2)* London: Peter Peregrinus Ltd.
- Doron, E., & Doron, M. A. (1992). Coherent wideband array processing. In *Acoustics, Speech, and Signal Processing, 1992. ICASSP-92., 1992 IEEE International Conference on*, 2, 497-500. IEEE.
- Evans, J. E., Johnson, J. R., & Sun, D. F. (1982). *Application of advanced signal processing techniques to angle of arrival estimation in ATC navigation and surveillance systems*, Tech rep., Lexington, MA: MIT Lincoln Laboratory.
- Gu, J. F., & Wei, P. (2007). Joint SVD of two cross-correlation matrices to achieve automatic pairing in 2-D angle estimation problems. *IEEE Antennas and Wireless Propagation Letters*, 6, 553-556.
- Haykin, S. (1985). *Array signal processing*. Englewood Cliffs, NJ, Prentice-Hall, Inc., 1985, 493 p. For individual items see A85-43961 to A85-43963.

- Hua, Y., Sarkar, T. K., & Weiner, D. (1989, August). L-shaped array for estimating 2-D directions of wave arrival. In *Circuits and Systems, 1989., Proceedings of the 32nd Midwest Symposium on*, 390-393. IEEE.
- Hwang, H. K., Aliyazicioglu, Z., Grice, M., & Yakovlev, A. (2008, March). Direction of arrival estimation using a root-MUSIC algorithm. In *Proceedings of the international Multi Conference of Engineers and Computer Scientists*, 2, 19-21.
- Ioannides, P., & Balanis, C. A. (2005). Uniform circular arrays for smart antennas. *IEEE Antennas and propagation magazine*, 47(4), 192-206.
- Jian, C., Shu-xun, W., & Xiao-li, W. (2006). New method for estimating two-dimensional direction of arrival based on L-shape array [J]. *Journal of Jilin University (Engineering and Technology Edition)*, 4, 030.
- Johnson, D. H. (1982). The application of spectral estimation methods to bearing estimation problems. *Proceedings of the IEEE*, 70(9), 1018-1028.
- Koca, S. (2015). *Positioning of radio signals via estimation of direction of arrival*. M.Sc. Thesis, Dokuz Eylül University, İzmir.
- Lau, B. K., & Leung, Y. H. (2000). A Dolph-Chebyshev approach to the synthesis of array patterns for uniform circular arrays. In *Circuits and Systems, 2000. Proceedings. ISCAS 2000 Geneva. The 2000 IEEE International Symposium on*, 1, 124-127. IEEE.
- Lee, A., Chen, L., Song, A., Wei, J., & Hwang, H. K. (2005, March). Simulation study of wideband interference rejection using adaptive array antenna. In *Aerospace Conference, 2005 IEEE* (1-6). IEEE.

- Liu, S., Yang, L., Li, D., & Cao, H. (2017). Subspace extension algorithm for 2D DOA estimation with L-shaped sparse array. *Multidimensional Systems and Signal Processing*, 28(1), 315-327.
- Ma, W. K., Hsieh, T. H., & Chi, C. Y. (2010). DOA estimation of quasi-stationary signals with less sensors than sources and unknown spatial noise covariance: A Khatri–Rao subspace approach. *IEEE Transactions on Signal Processing*, 58(4), 2168-2180.
- Mathews, C. P., & Zoltowski, M. D. (1994). Eigenstructure techniques for 2-D angle estimation with uniform circular arrays. *IEEE Transactions on signal processing*, 42(9), 2395-2407.
- Mathews, C. P., & Zoltowski, M. D. (1994). Performance analysis of the UCA-ESPRIT algorithm for circular ring arrays. *IEEE Transactions on Signal Processing*, 42(9), 2535-2539.
- Mubeen, S., Prasad, A.M., & Jhansi Rani, A. (2012). Smart Antenna for Doa using music and esprit. *IOSR Journal of Electronics and Communication Engineering (IOSRJECE)*, 1(1), 12-17.
- Pal, P., & Vaidyanathan, P. P. (2010). Nested arrays: A novel approach to array processing with enhanced degrees of freedom. *IEEE Transactions on Signal Processing*, 58(8), 4167-4181.
- Roy, R., & Kailath, T. (1989). ESPRIT-estimation of signal parameters via rotational invariance techniques. *IEEE Transactions on acoustics, speech, and signal processing*, 37(7), 984-995.
- Schmidt, R. (1986). Multiple emitter location and signal parameter estimation. *IEEE transactions on antennas and propagation*, 34(3), 276-280.

- Shan, T. J., Wax, M., & Kailath, T. (1985). On spatial smoothing for direction-of-arrival estimation of coherent signals. *IEEE Transactions on Acoustics, Speech, and Signal Processing*, 33(4), 806-811.
- Shapoury, A. (2007). *Ultra wideband antenna array processing under spatial aliasing*. Phd Thesis, Texas A&M University, USA.
- Tan, C. M., Landmann, M., Richter, A., Pesik, L., Beach, M. A., Schneider, C., & Nix, A. R. (2002). On the Application of Circular Arrays in Direction Finding Part II: Experimental evaluation on SAGE with different circular arrays. In *1st Annual COST 273 Workshop 5*, 29-30.
- Tayem, N., & Kwon, H. M. (2005). L-shape 2-dimensional arrival angle estimation with propagator method. *IEEE transactions on antennas and propagation*, 53(5), 1622-1630.
- Thummalapalli, S. (2012). *Wi-Fi Indoor Positioning*. M.Sc. Thesis, Halmstad University, School of Information Science, Computer and Electrical Engineering (IDE).
- Trinh, L. A., Duc Thang, N., Kim, D., Lee, S., & Chang, S. (2012). Application of matrix pencil algorithm to mobile robot localization using hybrid DOA/TOA estimation. *International Journal of Advanced Robotic Systems*, 9(6), 254.
- Wawak, F., Matia, F., Peignot, C., & Puente, E. A. (1999). A framework for the integration of perception and localization systems over mobile platforms. In *Progress in system and robot analysis and control design*, 495-504. Springer, London.
- Wax, M., & Sheinvald, J. (1994). Direction finding of coherent signals via spatial smoothing for uniform circular arrays. *IEEE transactions on antennas and propagation*, 42(5), 613-620.

Xia, M., & Du, R. (2006). New method of effective array for 2-D direction-of-arrival estimation. *International Journal of Innovative Computing, Information and Control*, 2(6), 1391-1397.

Zekavat, R., & Buehrer, R. M. (2011). *Handbook of position location: Theory, practice and advances* (27). New Jersey: Wiley-IEEE Press.

Zou, Z. (2012). *DSP-based System for 2D Wideband Acoustic Source Localization using UCA-ESPRIT*. M.Sc. Thesis, Hamburg University of Applied Sciences.



APPENDICES

ABBREVIATIONS

DOA	Direction-Of-Arrival
AOA	Angle-Of-Arrival
ML	Maximum Likelihood
ULA	Uniform Linear Array
UCA	Uniform Circular Array
LSA	L-Shaped Array
URA	Uniform Rectangular Array
SNR	Signal to Noise Ratio
RMSE	Root Mean Square Error
MCM	Mutual Coupling Matrix
MUSIC	Multiple Signal Classification
ESPRIT	Estimation of Signal Parameter via Rotational Invariance Techniques
SVD	Singular Value Decomposition
MVDR	Minimum Variance Distortionless Response
RTLS	Real Time Location Systems